Computational Intelligence in Electrical Engineering
Vol. 16, No. 1, 2025
pp. 75-90
Research Paper

Model-based Predictive Torque Control for Matrix Converter Fed Induction Motor Drive with Reactive Power Mitigation

Matin Nabizadeh[1], Pegah Hamedani[2*], Behzad Mirzaeian Dehkordi[3]

[1] MSc Student, Department of Electrical Engineering, Faculty of Engineering, University of Isfahan, Isfahan, Iran
m.nabizadeh@eng.ui.ac.ir
[2] Assistant Professor, Department of Railway Engineering and Transportation Planning, Faculty of Civil Engineering and Transportation, University of Isfahan, Isfahan, Iran
p.hamedani@eng.ui.ac.ir
[3] Professor, Department of Electrical Engineering, Faculty of Engineering, University of Isfahan, Isfahan, Iran
mirzaeian@eng.ui.ac.ir

Abstract :
Because of the inherent limitations of traditional AC-DC-AC converters, especially in electric motor drives, Matrix Converters (MCs), have attracted increasing attention as an alternative. Unlike traditional converters, MCs eliminate the necessity of a DC-link capacitor, support bidirectional power transfer, and enable precise reactive power management. These unique capabilities make MCs as a promising solution where advanced control is required. This study focuses on enhancing the performance of MCs by integrating Model Predictive Torque Control (MPTC) and uses a model predictive control (MPC) framework with a finite control set. The key aim is to control an induction motor (IM) drive fed through MC, exploiting the predictive nature of MPC to improve dynamic response and control flexibility over traditional approaches. The proposed controller's cost function includes terms for accurate torque and flux tracking, as well as grid-side reactive power regulation. To evaluate the performance, the MC-driven IM drive with the MPTC scheme was compared against a standard AC-DC-AC converter under identical operating scenarios. The results reveal superior torque tracking and adequate reactive power compensation by the MC. Notably, the MC-driven IM drive achieved approximately a 40% reduction in current Total Harmonic Distortion (THD) compared to the AC-DC-AC converter, and the grid-side reactive power was significantly mitigated compared to the conventional system.

Keywords: Model-based Predictive Control (MPC), Reactive Power Control, Torque Control, Induction Machine, Matrix Converter, AC-DC-AC Converter.

https://doi.org/10.22108/isee.2025.145445.1744

1. Introduction

Matrix Converters (MCs) are increasingly favored in various industrial applications as an alternative approach to regular AC-DC-AC converters that include DC-link capacitors [1]-[3]. Eliminating the DC-link capacitors results in a more compact, lightweight, and reliable converter design [4]-[5]. Furthermore, the MC features a relatively smaller number of switching elements while still enabling bidirectional power flow [4]-[5]. The ability to generate low-distortion input and output waveforms and control the grid-side power factor makes MCs highly attractive for various industrial applications [5].

Although MCs require more complex bidirectional switches and sophisticated protection circuits, they eliminate the bulky DC-link capacitor and rectifier stage, resulting in reduced system volume, improved reliability, and easier thermal management. From an economic perspective, the overall hardware cost of a matrix converter is generally comparable to that of a conventional voltage-source inverter (VSI) drive. In medium-power industrial applications (typically in the 5–10 kW range), the power stage of the MC may contribute to a slightly higher cost—approximately 15–20% more—due to the increased number of semiconductor devices and protection circuitry. However, this additional expense is offset mainly by eliminating the DC-link components, including large capacitors and rectifiers, which constitute a significant portion of the cost in conventional AC–DC–AC systems. Consequently, the total implementation cost of both converter types is similar. At the same time, the MC offers advantages such as lower maintenance, improved power factor, and reactive power mitigation, resulting in greater long-term cost-effectiveness.

Since the introduction of the MC topology, various control methods have been implemented to manage its operation [4]. The pulse-width modulation (PWM) [6]-[7] and space vector modulation (SVM) [8]-[9] strategies are the two most commonly used methods of controlling MCs. In addition, Direct Torque Control (DTC) has been employed for controlling electric motor drives powered by MCs [10]-[12]. However, when combined with the MC, these methods become complex. As a result, alternative control strategies have been proposed for MCs [13]-[16]. Even so, the main drawback of these control methods is their complexity, which makes them less suitable for industrial applications.

To achieve a superior dynamic response and address the complexity of controlling MCs, Model Predictive Control (MPC) has been proposed. Additionally, MPC is well-suited to handle the system's non-linear characteristics and constraints [17]-[18]. Several studies have reviewed the application of the MPC strategy for MCs [17]-[21].

Additionally, various MPC methods have been proposed for induction motor drives powered by an MC. The main MPC strategies developed for MCs include Predictive Current Control (PCC) [22]-[24], Predictive Torque Control (PTC) [25]-[27], Predictive Voltage Control (PVC) [28]-[29], and Predictive Power Control (PPC) [30]-[31]. Among these, PCC is the most widely used. Various objectives have been incorporated into the cost function of PCC, namely reactive power [32]-[34], Common-Mode (CM) Voltage [35], switching losses and efficiency [36].

Until now, most previous works on the MPC of MCs have concentrated on the PCC of resistive-inductive loads [37]-[38]. In [38], for example, a comparative assessment of Model Predictive Current Controlled (MPCC) MC against AC-DC-AC converters is given using an RL load. Grid-side reactive power control and switching frequency diminution were incorporated into the objective function, and the simulation results of the MC were compared with the traditional AC-DC-AC converters in similar conditions.

In [39], a comparative analysis of a direct matrix converter, a two-level interleaved DC-link back-to-back converter, and a three-level DC-link back-to-back converter for a 30-kW permanent magnet synchronous motor (PMSM) drive is presented. The research focuses on the volume and weight of passive components and electromagnetic interference (EMI) filters. The results highlight the trade-offs associated with each converter topology, providing insights into their relative advantages and limitations for high-performance motor drive applications.

In [40], the application of a new model predictive control (MPC) strategy for the control of an induction motor fed by a matrix converter is investigated. The given approach, termed Modulated Model Predictive Control (MMPC), integrates the key characteristics of a classical MPC with the SVM technique. This new control scheme preserves the main advantages of MPC —

including multi-objective control through a single feedback loop, fast transient response, straightforward incorporation of system non-linearities and constraints, and flexibility to accommodate additional system requirements — while introducing the benefits of fixed switching frequency operation and enhanced quality of the controlled waveforms. Simulation results demonstrating the performance of the proposed control method applied to a direct matrix converter induction motor drive are presented and discussed.

IMs are inherently non-linear systems due to their complex electromagnetic interactions, including magnetic saturation, slip-dependent behavior, and the coupling between stator and rotor flux linkages, which vary dynamically with load and operating conditions. These non-linearities make precise torque and speed control challenging, particularly under fast-changing or high-performance requirements. Traditional AC-DC-AC converters, while widely used in motor drive applications, rely on bulky DC link components and often face limitations in dynamic response, efficiency, and reactive power management. MCs, by contrast, offer a promising alternative because they discard the requirement of a DC-link, provide inherent bidirectional power flow, and enable direct control of active and reactive power at the same time.

Therefore, to fill the research gap in the case of MPC of MCs in electrical motor drives, this research focuses on controlling an IM drive fed through an MC using the MPTC strategy. Additionally, this paper examines the performance of the IM drive with the MPTC strategy by comparing the MC and AC-DC-AC converters. The novelty of this study lies in the integration of reactive power management within the predictive torque control framework for matrix converter-fed induction motors. Unlike conventional approaches that focus primarily on torque or current control, the proposed method simultaneously regulates torque, flux, and grid-side reactive power, offering a more comprehensive and flexible control solution. This allows the system to respond rapidly to dynamic load changes and reactive power demands without relying on bulky DC-link components, highlighting the practical advantages of matrix converters in high-performance drive applications.

The main contributions of this work to the literature are as follows:

- Introduction of a predictive torque control strategy for MC-fed induction motors with integrated reactive power management.
- Demonstration that the proposed MC-MPTC system outperforms conventional AC–DC–AC converters in terms of dynamic torque response, reactive power compensation, and elimination of bulky DC-link components.
- Provision of a detailed comparative analysis that can serve as a reference for future research in high-performance motor drives using matrix converters.

The remainder of this article is organized as follows: First, the MC is mathematically modeled. In Section 3, the mathematical model of an IM is explained. In Sections 4-5, the MPTC strategies for IM drive fed by MC and AC-DC-AC converters are described, respectively. Following that, simulation results of an IM drive with the MPTC method for MC and AC-DC-AC converters are presented. Finally, the conclusions are given.

2. Mathematical Model of an MC

Fig. 1 depicts the basic structure of an MC with an input L-C-R filter. The MC has nine bidirectional switches. The structure and switching conditions are described in [38].

The input filter state-space model can be expressed as [21]-[22]:

$$\dot{x}(t) = \boldsymbol{A}_c\,\boldsymbol{x}(t) + \boldsymbol{B}_c\,\boldsymbol{u}(t) \tag{1}$$

The state and input vectors are as follows:

$$\boldsymbol{x}(t) = \begin{bmatrix}\boldsymbol{v}_e(t)\\ \boldsymbol{i}_s(t)\end{bmatrix} \quad and \quad \boldsymbol{u}(t) = \begin{bmatrix}\boldsymbol{v}_s(t)\\ \boldsymbol{i}_e(t)\end{bmatrix} \tag{2}$$

$\boldsymbol{v}_s(t)$ and $\boldsymbol{i}_s(t)$ are the voltage and current space vectors at the power supply side, respectively.

In addition, $\boldsymbol{i}_e(t)$ and $\boldsymbol{v}_e(t)$ are the input current and input voltage space vectors of the MC, respectively.

$\boldsymbol{A}_c$ and $\boldsymbol{B}_c$, matrices of the state-space model are:

$$\boldsymbol{A}_c = \begin{bmatrix}0 & \frac{1}{C_f}\\ -\frac{1}{L_f} & -\frac{R_f}{L_f}\end{bmatrix}, \boldsymbol{B}_c = \begin{bmatrix}0 & -\frac{1}{C_f}\\ \frac{1}{L_f} & 0\end{bmatrix} \tag{3}$$

R_f, L_f, and C_f are the filter resistor, inductor, and capacitor, respectively.

Using (1), the discrete model of the input filter can be written as [37]:

$$\boldsymbol{i}_s(k+1) = \boldsymbol{A}_q(2,1)\,\boldsymbol{v}_e(k) + \boldsymbol{A}_q(2,2)\,\boldsymbol{i}_s(k) + \boldsymbol{B}_q(2,1)\,\boldsymbol{v}_s(k) + \boldsymbol{B}_q(2,2)\,\boldsymbol{i}_e(k) \tag{4}$$

where

$$\boldsymbol{A}_q = e^{\boldsymbol{A}_c T_s}, \quad \boldsymbol{B}_q = \int_0^{T_s} e^{\boldsymbol{A}_c (T_s - \tau)} \boldsymbol{B}_c d\tau \tag{5}$$

T_s is the sampling time.

The output voltage of the MC is obtained from the input voltage as follows [21]-[22]:

$$\boldsymbol{v}_{oN}(t) = \boldsymbol{T} \cdot \boldsymbol{v}_e(t) \tag{6}$$

where $\boldsymbol{v}_{oN}(k)$ and $\boldsymbol{v}_e(k)$ are the output voltage and input voltage of the MC relative to source mid-point N, respectively:

$$\boldsymbol{v}_{oN}(t) = \begin{bmatrix} v_{aN}(t) \\ v_{bN}(t) \\ v_{cN}(t) \end{bmatrix} \quad and \quad \boldsymbol{v}_e = \begin{bmatrix} v_{eu}(t) \\ v_{ev}(t) \\ v_{ew}(t) \end{bmatrix} \tag{7}$$

In (6), $\boldsymbol{T}$ is the transformation matrix:

$$\boldsymbol{T} = \begin{bmatrix} S_{ua} & S_{va} & S_{wa} \\ S_{ub} & S_{vb} & S_{wb} \\ S_{uc} & S_{vc} & S_{wc} \end{bmatrix} \tag{8}$$

where S_{xy} is the switching condition of each bidirectional switch. As depicted in Fig. 1, x stands for the MC input phase ($x \in \{u, v, w\}$) and y stands for the MC output phase ($y \in \{a, b, c\}$).

For short-circuit avoidance, the switches in an output phase cannot be simultaneously turned on [19]:

$$S_{uy} + S_{vy} + S_{wy} = 1 \quad \forall \quad y \in \{a, b, c\} \tag{9}$$

Using (6), the phase voltages of the stator can be computed:

$$\boldsymbol{V}_o(t) = \begin{bmatrix} v_{an}(t) \\ v_{bn}(t) \\ v_{cn}(t) \end{bmatrix} = \begin{bmatrix} v_{aN}(t) - v_{nN}(t) \\ v_{bN}(t) - v_{nN}(t) \\ v_{cN}(t) - v_{nN}(t) \end{bmatrix} \tag{10}$$

v_{nN} can be written as [19]:

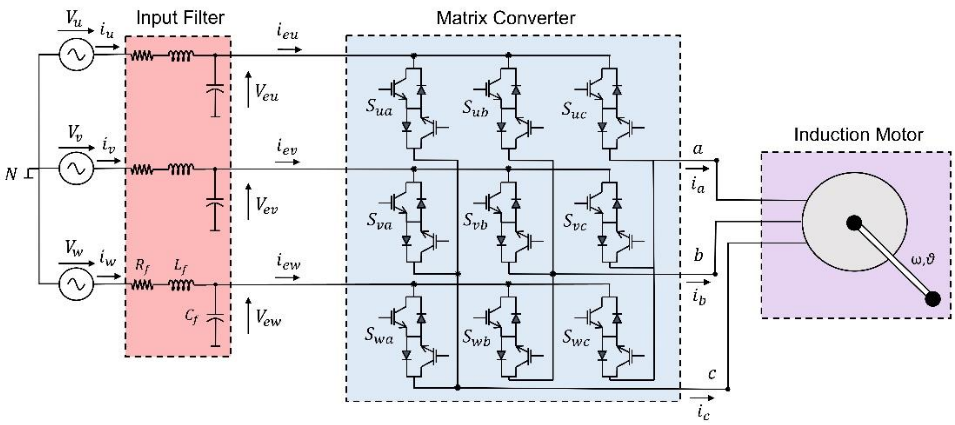

Fig. 1. Structure of a three-phase MC

$$v_{nN}(t) = \frac{v_{aN}(t) + v_{bN}(t) + v_{cN}(t)}{3} \tag{11}$$

where *n* is the neutral point of the IM.

The input current can be derived from the output current of the MC as [22]:

$$\boldsymbol{i}_e(t) = \boldsymbol{T}^T \cdot \boldsymbol{i}_o(t) \tag{12}$$

$\boldsymbol{i}_e(k)$ and $\boldsymbol{i}_o(k)$ are the input current and output current of the MC, respectively:

$$\boldsymbol{i}_e(t) = \begin{bmatrix} i_{eu}(t) \\ i_{ev}(t) \\ i_{ew}(t) \end{bmatrix} \quad and \quad \boldsymbol{i}_o(t) = \begin{bmatrix} i_a(t) \\ i_b(t) \\ i_c(t) \end{bmatrix} \tag{13}$$

The transformation matrix is the same as (8).

3. Discrete-Time Modeling of an IM

The MPC strategy needs the discrete-time model of the load. For IMs, the discrete-time model has been given in the literature [41]. The rotor and stator flux can be predicted in (*k*+1)-th step time [41]:

$$\boldsymbol{\psi}_s(k+1) = \boldsymbol{\psi}_s(k) + T_s \boldsymbol{V}_o(k) - R_s T_s \boldsymbol{i}_o(k) \tag{14}$$

$$\boldsymbol{\psi}_r(k+1) = \frac{L_r}{L_s} \boldsymbol{\psi}_s(k+1) + \boldsymbol{i}_o(k) \left(L_m - \frac{L_r L_s}{L_m} \right) \tag{15}$$

where $\boldsymbol{V}_o$ and $\boldsymbol{i}_o$ are the voltage and current vectors of the stator, which can be written in α-β coordinates, respectively.

$$\boldsymbol{V}_o = V_\alpha + jV_\beta \;,\;\; \boldsymbol{i}_o = i_\alpha + ji_\beta \tag{16}$$

where $\boldsymbol{\psi}_s$ and $\boldsymbol{\psi}_r$ are the stator flux and rotor flux vectors, respectively. L_S, L_r, and L_m are the stator, rotor, and magnetizing inductances, respectively. T_s is the sampling time.

Using (14)-(15), the stator current vector in the (k+1)-th sampling time can be computed as [41]:

$$\boldsymbol{i}_o(k+1) = \left(1 - \frac{T_s}{\tau_\sigma}\right)\boldsymbol{i}_o(k) + \frac{T_s}{\tau_\sigma}\left\{\frac{1}{R_\sigma}\left[\left(\frac{K_r}{\tau_r} - j\,K_r\omega_r\right)\boldsymbol{\psi}_r(k+1) + \boldsymbol{V}_o(k)\right]\right\} \tag{17}$$

where $R_\sigma = R_s + R_r K_r^2,\; K_r = \frac{L_m}{L_r}$, $\sigma = 1 - \frac{L_m^2}{L_s\,L_r}$, $\tau_\sigma = \frac{\sigma\,L_s}{R_\sigma}$.

From (14) and (17), the electromagnetic torque in the (k+1)-th sampling time can be calculated as [41]:

$$T(k+1) = \frac{3}{2} p\, Im\{\bar{\boldsymbol{\psi}}_s(k+1)\boldsymbol{i}_o(k+1)\} \tag{18}$$

where p is the number of pole pairs, and $\bar{\boldsymbol{\psi}}_s$ is the complex conjugate value of $\boldsymbol{\psi}_s$.

4. MPTC of an IM Drive Fed by an MC

Fig. 2 illustrates the block diagram of the MPTC of an IM fed through the MC. For all 27 switching conditions of the MC, the motor current must be computed in the next sampling instant. The optimum switching condition for minimizing the objective function is chosen and utilized in the next sampling instant in the converter. In Fig. 3, the overall flowchart of the MPTC for an IM drive fed by an MC is given.

The cost function is structured as follows:

$$g(k+1) = g_h(k+1) + \lambda_Q\, g_Q(k+1) \tag{19}$$

λ_Q *is* the weighting factor that adjusts the reactive power. g_h can be shown as [37]:

$$g_h = |T^* - T(k+1)| + \lambda_\psi |\boldsymbol{\psi}_s^* - \boldsymbol{\psi}_s(k+1)| \tag{20}$$

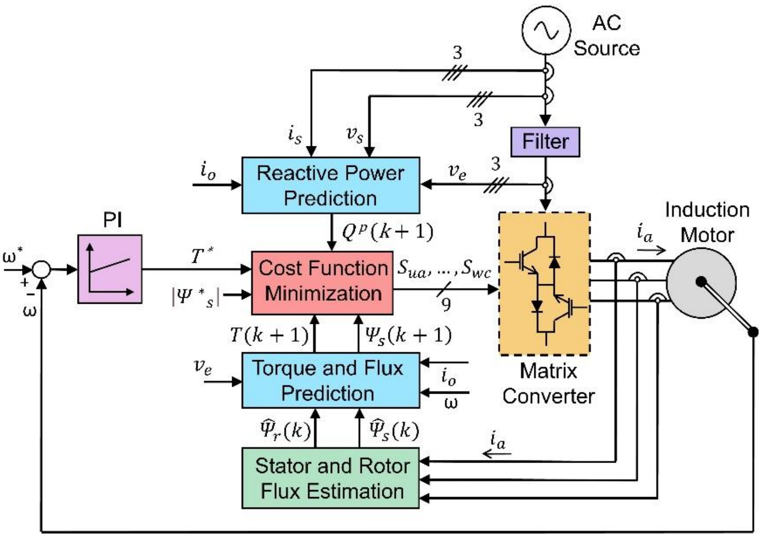

Fig. 2. Diagram of the MPTC for IM drive fed by an MC

where λ_ψ is the flux and torque regulation weighting factor and can be characterized as the nominal torque and nominal stator flux ratio [37]:

$$\lambda_\psi = \frac{T_n}{|\psi_{s_n}|} \tag{21}$$

Moreover, g_Q can be written as [38]:

$$g_Q = |Q^* - Q(k+1)| \tag{22}$$

in which Q^* is the desired reactive power value.

Assuming $\boldsymbol{v}_s(k+1) \approx \boldsymbol{v}_s(k)$, the grid-side reactive power $Q(k+1)$ can be computed as [38]:

$$\begin{aligned} Q(k+1) &= Im\{\boldsymbol{v}_s(k+1)\cdot\bar{\boldsymbol{\imath}}_s(k+1)\} \\ &= v_{s\beta}(k+1)\, i_{s\alpha}(k+1) \\ &\quad - v_{s\alpha}(k+1)\, i_{s\beta}(k+1) \end{aligned} \tag{23}$$

$\boldsymbol{v}_s(k+1)$ and $\boldsymbol{i}_s(k+1)$ are the measured voltages and currents at the power supply side, respectively, and can be calculated as:

$$v_{s\alpha} = \frac{2}{3}\left(v_{sa} - \frac{1}{2}\,v_{sb} - \frac{1}{2}\,v_{sc}\right) \tag{24}$$

$$v_{s\beta} = \frac{2}{3}\left(\frac{\sqrt{3}}{2}\,v_{sb} - \frac{\sqrt{3}}{2}\,v_{sc}\right) \tag{25}$$

$$i_{s\alpha} = \frac{2}{3}\left(i_{sa} - \frac{1}{2}\, i_{sb} - \frac{1}{2}\, i_{sc}\right) \quad (26)$$

$$i_{s\beta} = \frac{2}{3}\left(\frac{\sqrt{3}}{2}\, i_{sb} - \frac{\sqrt{3}}{2}\, i_{sc}\right) \quad (27)$$

5. MPTC of IM Drive Fed by an AC-DC-AC Converter

The general schematic of an IM drive fed by an AC-DC-AC converter is presented in Fig. 4. Dynamic braking has been considered in reverse motoring conditions. In Fig. 5, the block diagram of the MPTC of an IM fed through the AC-DC-AC converter is shown. In this structure, the reactive power cannot be controlled. Therefore, the cost function consists of torque and flux magnitude errors, according to (20). Moreover, the DC-link voltage is measured and utilized for calculating the stator voltage vectors in (14) and (17). Fig. 6 illustrates the flowchart of the MPTC for an IM drive fed by the AC-DC-AC converter.

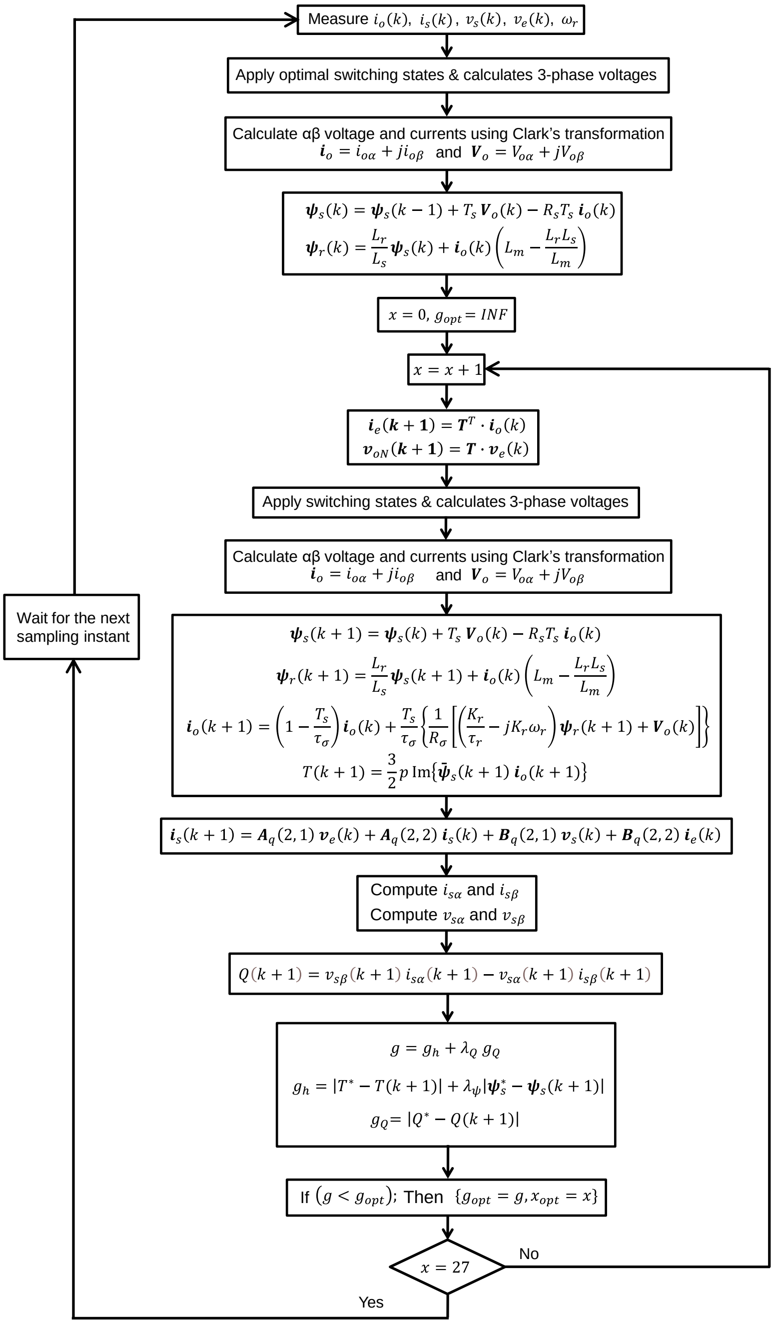

Fig. 3. Flowchart of the MPTC for IM drive fed by an MC

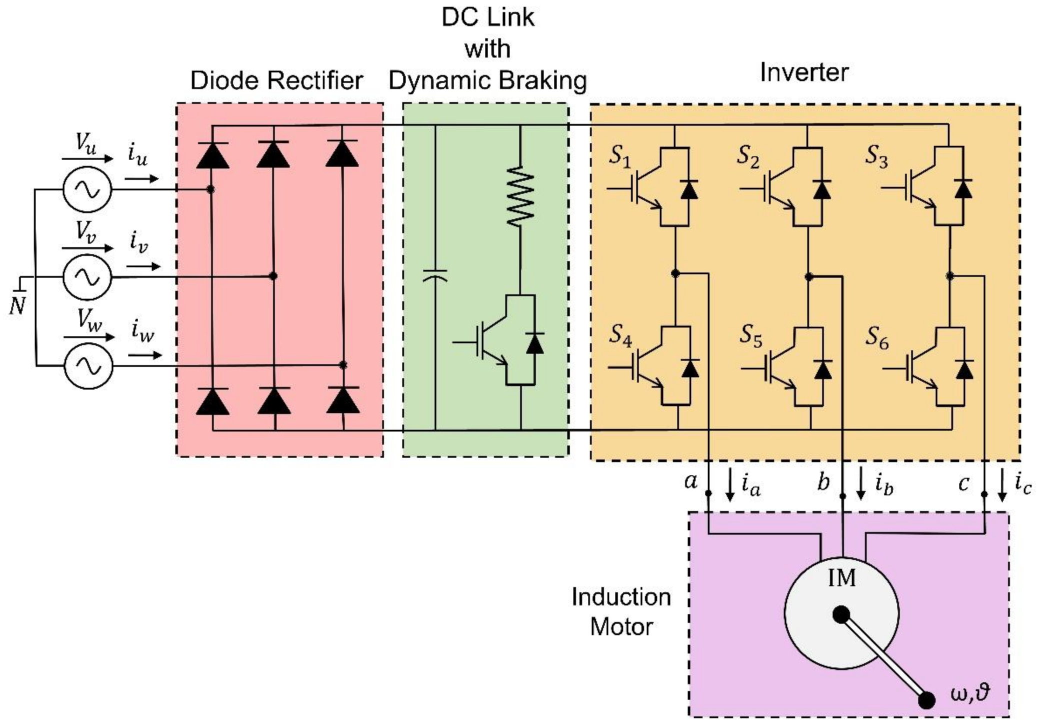

Fig. 4. Structure of an IM drive fed by an AC-DC-AC converter

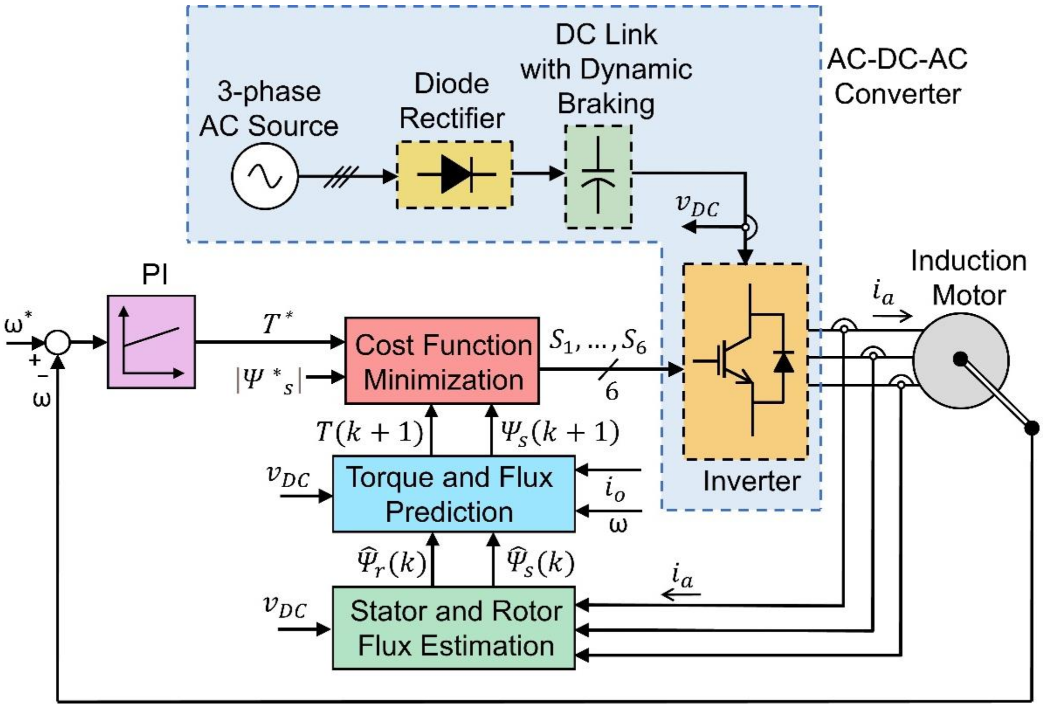

Fig. 5. Diagram of the MPTC for an IM drive fed by an AC-DC-AC converter

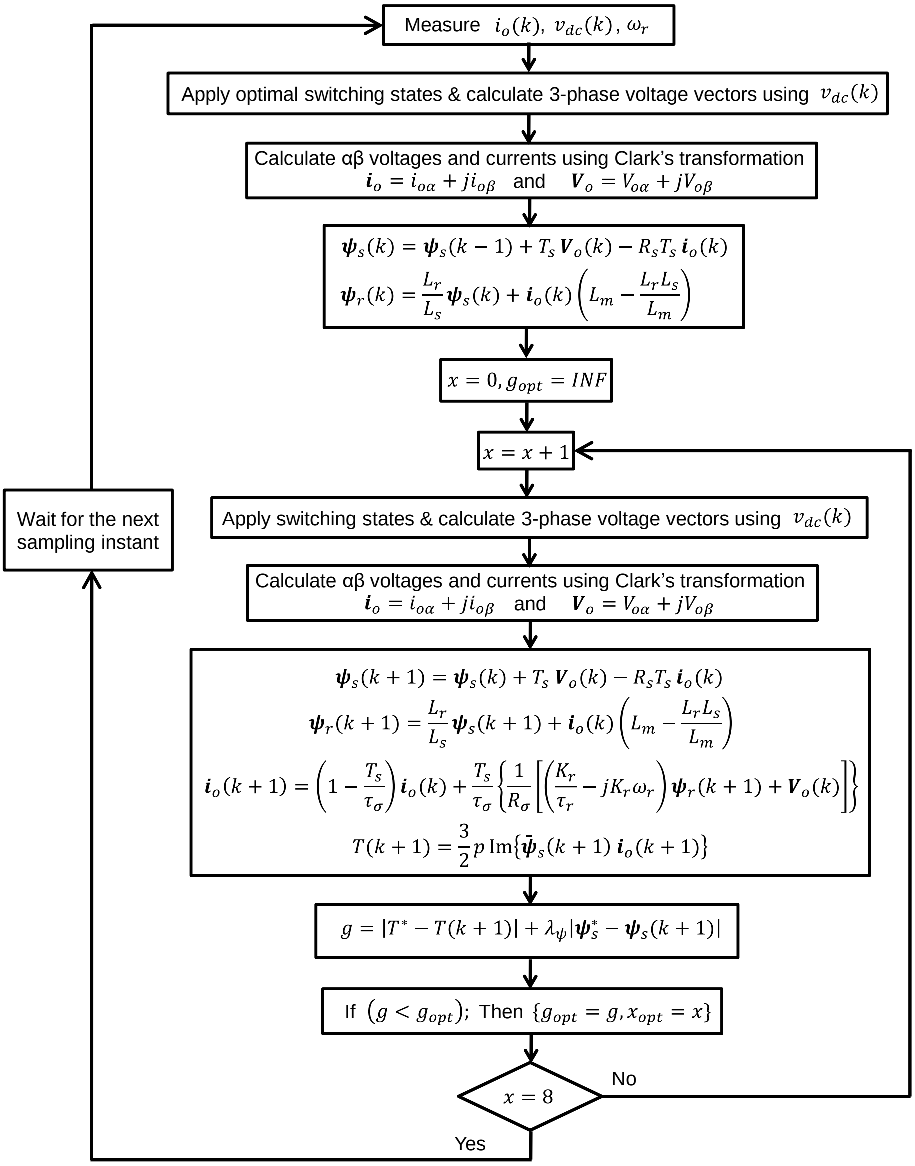

Fig. 6. Flowchart of the MPTC for IM drive fed by an AC-DC-AC converter

6. Results and Discussion

This section presents the detailed simulation results of the proposed MPTC approach used on an IM drive fed by an MC. The parameters used in the simulations are listed in the Appendix. The reference speed is changed from 375 rpm to -375 rpm at t = 2.5 s, while the IM starts at no load. An 18 Nm load torque is applied to the drive at t = 1.5 s.

Fig. 7(a) shows the reference and actual speed of the induction motor. It can be observed that the motor responds rapidly to both the speed reversal at 2.5 s and the load application at 1.5 s, demonstrating the fast dynamic response and robustness of the proposed MPTC strategy. The speed remains stable during transient events, confirming that the control effectively maintains the reference trajectory.

Fig. 7(b) presents the electromagnetic torque T_e alongside the applied load torque T_{load}. The electromagnetic torque accurately tracks the load, reflecting the MPTC's ability to respond to sudden load changes and motor startup conditions. Zoomed views highlight minor torque ripples, which are inherent to predictive control due to discrete switching, yet remain within acceptable limits for high-performance drives.

Fig. 7(c) shows the stator currents of the IM. The currents closely follow the load conditions, with clear correspondence between applied torque and current amplitude. During transient events such as load application and speed reversal, the current waveforms remain well-regulated without excessive overshoot. This indicates precise current control by the MPTC algorithm.

Fig. 7(d) displays both the source current i_u and the input current of the MC i_{eu}. The results show that the source current is significantly smoother due to the L–C–R filter, highlighting the MC's capability to maintain high power quality at the grid side. The magnified views reveal minor high-frequency components associated with switching, which are effectively filtered to avoid adverse effects on the supply.

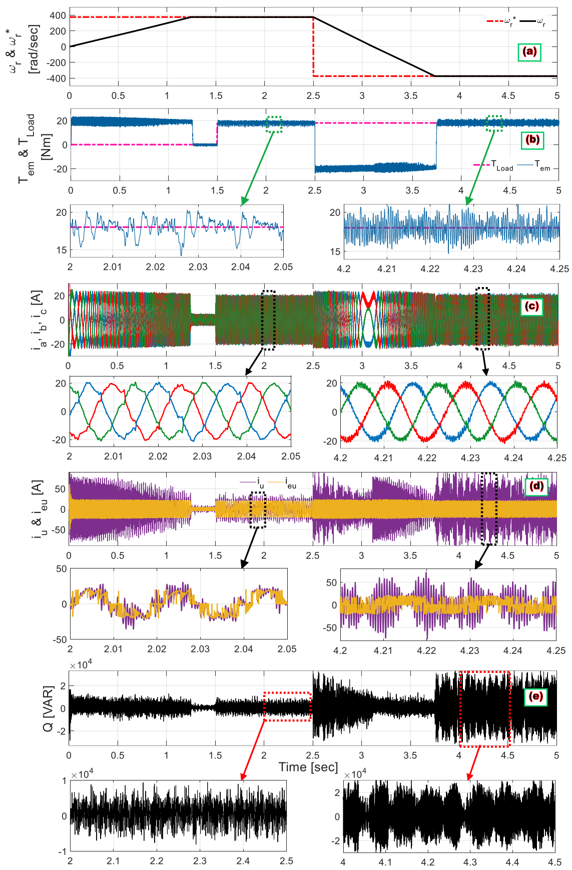

Fig. 7. Simulation results of the MPTC of IM drive with MC for λ_Q=0: (a) reference and actual speed; (b) load and electromagnetic torque; (c) stator currents; (d) i_u and i_{eu}; (e) reactive power

Fig. 7(e) illustrates the instantaneous supply side reactive power. For λ_Q = 0, the input power factor is not actively controlled, resulting in reactive power fluctuations corresponding to load and speed changes. The observed reactive power profile provides a baseline for assessing the impact of non-zero λ_Q in subsequent simulations, where the controller actively mitigates reactive power.

Overall, the results demonstrate the comprehensive performance of the proposed MPTC strategy, including fast torque tracking, stable speed response, precise current regulation, and power quality improvement at the supply side. The minor torque and current ripples observed are a typical trade-off in predictive control but do not compromise overall system performance. Furthermore, the figures provide insight into the interplay between load dynamics, motor response, and supply-side behavior, which is essential for validating the effectiveness of the proposed approach and comparing it to conventional AC–DC–AC converters in subsequent analyses.

In the MPTC method for MC, the grid-side reactive power can be moderated by raising the weighting factor λ_Q in the objective function of MPTC. Fig. 8 illustrates the simulation results of the IM drive fed by the matrix converter using the proposed MPTC approach for λ_Q= 0.0006. By introducing the reactive power weighting term into the MPTC cost function, the controller actively moderates the grid-side reactive power while maintaining precise torque and speed regulation.

As shown in Fig. 8(a)–(b), the motor speed accurately follows the reference profile during acceleration, steady-state, and speed reversal, confirming that the inclusion of λ_Q does not heavily affect the dynamic performance of the drive. The electromagnetic torque shown in Fig. 8(b) closely tracks the reference torque, with smooth transient responses under load application and reversal conditions. This demonstrates that the proposed controller maintains robust torque performance even when reactive power control is activated.

In Fig. 8(c)–(d), the stator currents and input currents of the MC exhibit smoother and more balanced waveforms compared to the λ_Q = 0 case. The grid-side currents remain nearly sinusoidal, and their phase shift relative to the supply voltage is substantially reduced. This indicates a marked improvement in the input power factor, confirming the successful mitigation of reactive power. The L–C–R filter continues to play an essential role in shaping the input current waveform and reducing high-frequency switching components.

The effectiveness of the reactive power control is clearly visible in Fig. 8(e), which shows the instantaneous grid-side reactive power. Compared with Fig. 7(e), the amplitude of the reactive power oscillations is notably diminished, and the average reactive power is nearly zero. This verifies that the proposed MPTC scheme with λ_Q = 0.0006 achieves near-unity power factor operation.

However, it can also be noted that as λ_Q increases, a trade-off emerges: while reactive power is reduced, the current total harmonic distortion (THD) slightly increases due to the controller's prioritization of reactive power minimization over current waveform optimization. Despite this, the resulting current quality remains within acceptable limits for industrial applications.

Overall, these results confirm that the inclusion of λ_Q in the MPTC cost function effectively enables real-time control of reactive power without significantly degrading the dynamic performance or current quality of the IM drive. The proposed method provides a practical balance between torque accuracy, reactive power mitigation, and input current distortion, demonstrating the flexibility and adaptability of the predictive control framework for matrix converter-fed drives.

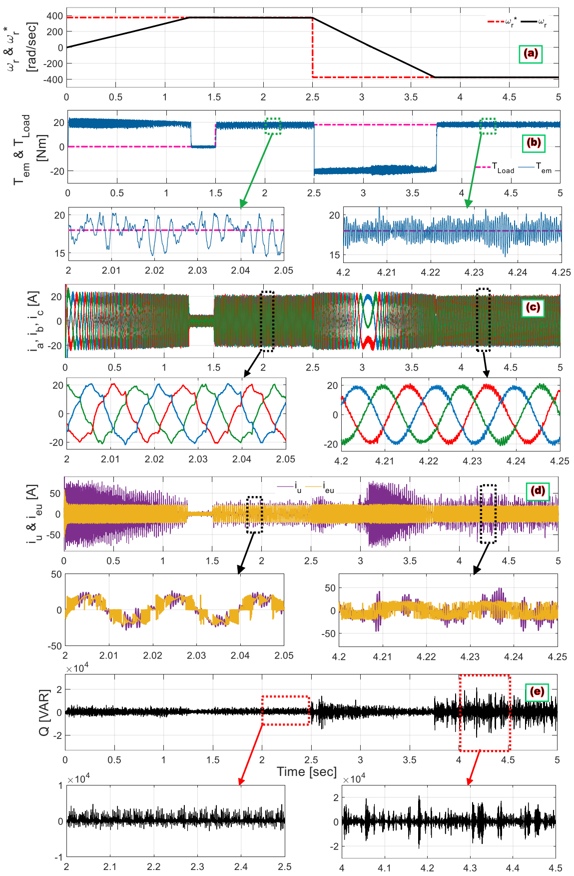

Fig. 8. Simulation results of the MPTC of an IM drive with an MC for λ_Q=0.0006: (a) reference and actual speed; (b) load and electromagnetic torque; (c) stator currents; (d) i_u and i_{eu}; (e) reactive power

Next, the performance of an IM drive supplied by the AC-DC-AC converter using the MPTC is presented. Fig. 9 presents the simulation results of the IM drive supplied by the conventional AC–DC–AC converter using the same MPTC strategy for fair comparison with the matrix converter-based system. Figs. 9(a)–(c) illustrate the actual and reference speed, electromagnetic and load torque, and stator currents, respectively. It is observed that the IM achieves a rapid dynamic speed response that remains stable during acceleration, deceleration, and reversal of rotation. The electromagnetic torque in Fig. 9(b) accurately follows the reference, effectively handling load application and removal events with minimal overshoot. Similarly, the stator currents shown in Fig. 9(c) correspond well with the mechanical load variations, indicating good current control performance of the predictive strategy.

Despite this satisfactory performance, several important distinctions can be observed when comparing the AC–DC–AC converter with the matrix converter configuration. The AC–DC–AC converter relies on a DC-link capacitor, which provides energy buffering but introduces additional passive components that increase system size, weight, and losses. Furthermore, due to the presence of separate rectifier and inverter stages, the converter exhibits a less favorable input current profile, and the grid-side reactive power cannot be directly regulated through the MPTC cost function. Consequently, the overall power factor is lower, and the reactive power oscillations are larger compared to the MC-based system.

In terms of current quality, the AC–DC–AC converter shows slightly higher total harmonic distortion (THD) at the supply side, mainly due to the diode rectifier and the DC-link voltage ripple. However, the DC-link also helps in stabilizing the system voltage and reducing the neutral-to-ground voltage variations, which provides a more constant operating condition for the inverter stage.

Overall, while the AC–DC–AC converter demonstrates acceptable torque and speed control performance under the MPTC strategy, it lacks the capability for direct reactive power control and bidirectional power flow. The matrix converter, in contrast, achieves comparable or superior dynamic performance with reduced passive components, lower THD, and controllable input power factor, confirming its advantage as a more compact and efficient alternative for high-performance IM drives.

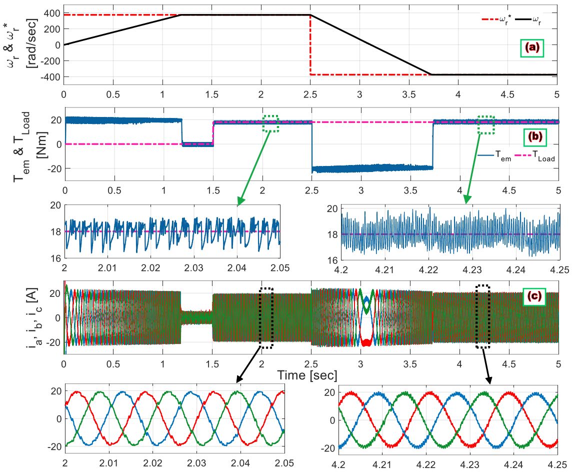

Fig. 9. Simulation results of the MPTC of an IM drive with an AC-DC-AC converter: (a) reference and actual speed; (b) load and electromagnetic torque; (c) stator currents

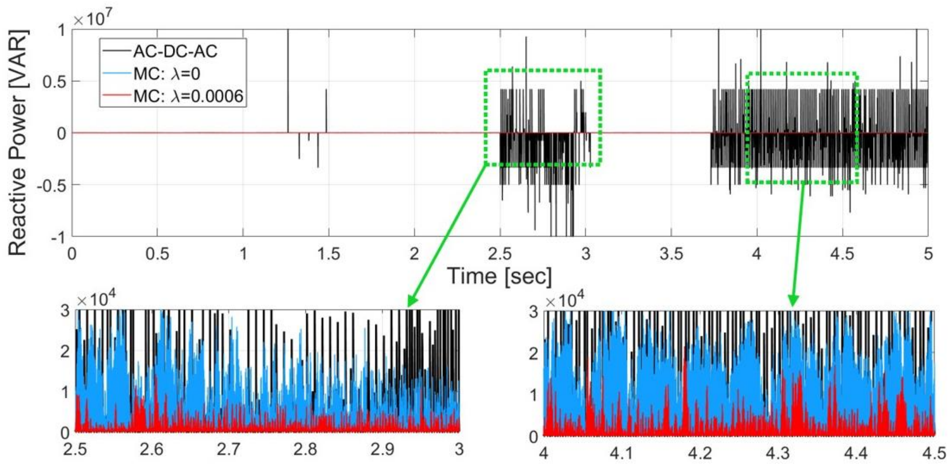

Fig. 10. Comparison of the reactive power in an IM drive fed by an MC and AC-DC-AC converter

Fig. 10 compares the instantaneous grid-side reactive power for three configurations: the AC–DC–AC converter, the MC with $\lambda_Q = 0$, and the MC with $\lambda_Q = 0.0006$. As seen in the figure, the reactive power in the IM drive supplied by the AC–DC–AC converter is significantly higher and fluctuates over a wide range, indicating the absence of reactive power control capability. This behavior results from the unidirectional nature of the diode rectifier stage and the lack of direct interaction between the grid and inverter control loops, which prevents active regulation of the input power factor.

In contrast, the IM drive fed by the matrix converter exhibits considerably lower reactive power variations even without incorporating the reactive power term ($\lambda_Q = 0$) in the MPTC cost function. This reduction is mainly attributed to the inherent bidirectional power flow capability of the MC and the elimination of the DC-link capacitor, which allows instantaneous power flow between the grid and the motor.

When the reactive power term is introduced into the cost function ($\lambda_Q = 0.0006$), the improvement becomes even more evident. The grid-side reactive power is substantially mitigated, and the waveform remains tightly centered around zero, indicating near-unity power factor operation. The lower subplots in Fig. 10 provide a magnified view of two transient intervals, clearly showing that the proposed MPTC approach with $\lambda_Q = 0.0006$ effectively suppresses reactive power oscillations under both steady-state and dynamic conditions.

These results confirm that integrating the reactive power weighting factor into the predictive control algorithm enables precise real-time management of the grid-side reactive power without compromising torque or speed performance. Consequently, the proposed MPTC-based MC system achieves a superior balance between dynamic response, power quality, and converter efficiency compared to the conventional AC–DC–AC topology.

Table 1 compares the electromagnetic torque ripple of the IM drive for both the AC–DC–AC converter and the MC with different load conditions. It is evident that the MC exhibits lower torque ripple than the conventional converter across all cases. At half-load (T_{Load} =9 Nm), the torque ripple is reduced from 2.23 Nm (AC–DC–AC) to 2.05 Nm (MC, λ_Q = 0) and further to 2.03 Nm (MC, λ_Q = 0.0006), corresponding to a 9% reduction compared with the conventional converter. Under full-load conditions (T_{Load} =18 Nm), the torque ripple decreases from 3.95 Nm (AC–DC–AC) to 3.26 Nm (MC, λ_Q = 0) and 2.51 Nm (MC, λ_Q = 0.0006), which represents an overall reduction of approximately 36.5%. The improvement becomes more significant at higher torque levels, showing that the predictive control strategy effectively suppresses electromagnetic torque oscillations under dynamic loading.

Table (1): Comparison of the torque ripple [Nm] in an IM drive fed by an AC-DC-AC converter and an MC.

	AC-DC-AC Converter	MC	
		$\lambda_Q = 0$	$\lambda_Q = 0.0006$
T_{Load}=9 [Nm]	2.23	2.05	2.03
T_{Load}=18 [Nm]	3.95	3.26	2.51

Table 2 and Fig. 11 present a detailed comparison of the stator current THD for the IM drive controlled by MPTC when supplied by either an AC–DC–AC converter or an MC. The data clearly show that the MC consistently produces lower current distortion across all load conditions.

At half-load (T_{Load} = 9 Nm), the average THD is reduced from 13.96% in the AC–DC–AC converter to 10.30% in the MC without reactive-power weighting (λ_Q = 0) and further to 9.22% when λ_Q = 0.0006, corresponding to an overall 34% reduction. The minimum and maximum THD values also decrease from 10.05%/23.06% to 8.63%/11.09%, confirming that the proposed control scheme effectively suppresses both steady-state and transient harmonic distortions.

Under full-load operation (T_{Load} = 18 Nm), the THD improvement is even more significant. The average THD drops from 12.91% in the AC–DC–AC converter to 7.57% in the MC without reactive-power control and to 7.67% when λ_Q = 0.0006—an overall reduction of approximately 41%. Similarly, the minimum and maximum THD values decline from 7.94%/24.74% to 5.43%/12.74%.

These results demonstrate that the matrix converter, in combination with the MPTC algorithm, delivers markedly improved current quality by generating near-sinusoidal stator currents with lower harmonic content. The elimination of the DC-link capacitor and the direct bidirectional AC–AC power conversion allow the MC to avoid low-frequency oscillations typical of back-to-back converters. Furthermore, the inclusion of the reactive-power weighting factor (λ_Q) enables additional fine-tuning of grid-side power quality without degrading the dynamic torque response.

Consequently, the proposed MPTC-based MC topology achieves superior harmonic performance and enhanced power-quality characteristics compared with the conventional AC–DC–AC converter, validating its effectiveness for high-performance induction-motor drive systems.

Table (2): Comparison of the current THD [%] in an IM drive fed by an AC-DC-AC converter and an MC.

		AC-DC-AC Converter	MC	
			$\lambda_Q = 0$	$\lambda_Q = 0.0006$
T_{Load}=9 [Nm]	Min	10.05	8.90	8.63
	Max	23.06	11.96	11.09
	Avg	**13.96**	**10.30**	**9.22**
T_{Load}=18 [Nm]	Min	7.94	6.73	5.43
	Max	24.74	12.75	12.74
	Avg	**12.91**	**7.57**	**7.67**

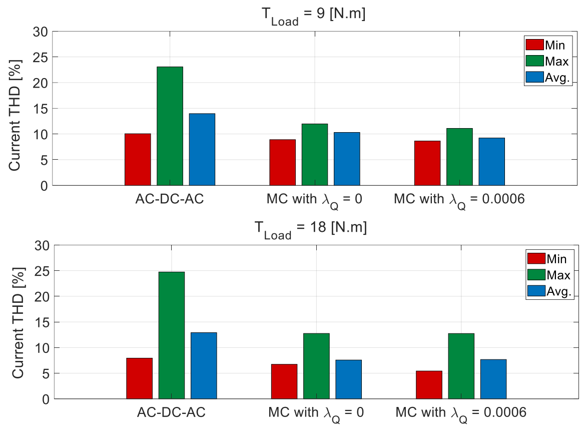

Fig. 11. Comparison of the current THD [%] in an IM drive fed by an AC-DC-AC converter and an MC

7. Conclusion

This work has presented a Model Predictive Torque Control (MPTC) strategy for induction motor drives fed by a matrix converter, successfully achieving precise electromagnetic torque regulation while simultaneously providing effective grid-side reactive power control. The proposed approach was thoroughly evaluated and compared against a conventional AC–DC–AC converter under identical operating conditions. Simulation results demonstrate that the matrix converter, when controlled using the proposed MPTC strategy, delivers superior dynamic performance, nearly complete mitigation of reactive power on the supply side, and a substantial reduction in current Total Harmonic Distortion (THD) compared to traditional AC–DC–AC systems. These findings confirm the success of the predictive control framework in managing both torque and power quality objectives in a single unified control structure. While the study demonstrates significant benefits, it acknowledges certain limitations. The results are based on simulation studies under balanced three-phase supply conditions and medium-power motors, which may not fully capture the behavior under unbalanced or non-ideal grid conditions. Experimental validation on real hardware is planned for future work to confirm the robustness and potential of the proposed strategy under practical operating scenarios. Additionally, extending the method to multi-motor systems or renewable energy interfaces could further increase its applicability, while incorporating advanced observer designs or machine learning-based predictive models may enhance computational efficiency and control accuracy. In summary, this work advances the state-of-the-art by providing a practical and effective MPTC strategy for matrix converter-driven induction motor drives, combining precise torque regulation with reactive power management, improved power quality, and high dynamic performance. The findings provide a solid foundation for future research and industrial applications in high-performance motor drives and power electronic systems.

Appendix

Table (A1): IM Parameters

Parameter		Value
IM	J	0.062 [Kg.m2]
	P	1
	$S_{f\text{-}nom}$	0.71 [Wb]
	T_{nom}	20 [N.m]
	L_m	170 [mH]
	L_s	175 [mH]
	L_r	175 [mH]
	R_s	1.2 [Ohm]
	R_r	1 [Ohm]

Table (A2): MPTC Parameters

Parameter		Value
Solver Parameters	T_{sim}	5 [μsec]
	T_s	40 [μsec]
PI Gain	K_p	3.016
	K_i	0.141
Weighting Factor	λ_ψ	28.17

Table (A3): MC and AC-DC-AC Parameters

Parameter		Value
Input Filter	L_f	400 [μH]
	R_f	0.5 [Ohm]
	C_f	21 [μF]
Input Source	V_s	320 [V]
	ω_s	2π50 [rad/s]
DC Link	$C_{DC\text{-}Link}$	2200 [μF]
	V_{DC}	520 [V]

Acknowledgment

The authors thank the anonymous reviewers for their careful reading of our manuscript and their informative comments and suggestions.

References

[1] L. Empringham, J. W. Kolar, J. RodrigueFz, P. W. Wheeler, J. C. Clare, "Technological issues and industrial application of matrix converters: A review", IEEE Trans. Ind. Electron., Vol. 60, No. 10, pp. 4260–4271, 2013. https://doi.org/10.1109/TIE.2012.2216231

[2] J. Rodriguez, M. Rivera, J. W. Kolar, P. W.

Wheeler, "A review of control and modulation methods for matrix converters", IEEE Trans. Ind. Electron., Vol. 59, No. 1, pp. 58–70, 2012. https://doi.org/10.1109/TIE.2011.2165310

[3] S. Muller, U. Ammann, S. Rees, "New time-discrete modulation scheme for matrix converters", IEEE Transactions on Industrial Electronics, Vol. 52, No. 6, pp. 1607-1615, December 2005. https://doi.org/10.1109/TIE.2005.858713

[4] P. W. Wheeler, J. Rodriguez, J. C. Clare, L. Empringham, A. Weinstein, "Matrix converters: A technology review", IEEE Transactions on Industrial Electronics, Vol. 49, No. 2, pp. 276-288, April 2002. https://doi.org/10.1109/41.993260

[5] T. N. Mir, B. Singh, A. H. Bhat, "FS-MPC-based speed sensorless control of matrix converter fed induction motor drive with zero common mode voltage", In IEEE Transactions on Industrial Electronics, Vol. 68, No. 10, pp. 9185-9195, October 2021. https://doi.org/10.1109/TIE.2020.3020031

[6] P. Kiatsookkanatorn, S. Sangwongwanich, N. Watjanatepin, "Realization of SVM methods with carrier-based dipolar PWM for matrix converters", In IEEE Access, Vol. 12, pp. 68531-68544, 2024. https://doi.org/10.1109/ACCESS.2024.3399078

[7] Y. Li, H. Tian, Y. R. Li, "Matrix-based approach for open-circuit fault-tolerant analysis and PWM design of active neutral-point-clamped converters", In IEEE Transactions on Power Electronics, Vol. 37, No. 12, pp. 14706-14719, December 2022. https://doi.org/10.1109/TPEL.2022.3193972

[8] A. Tsoupos, V. Khadkikar, "A novel SVM technique with enhanced output voltage quality for indirect matrix converters", In IEEE Transactions on Industrial Electronics, Vol. 66, No. 2, pp. 832-841, February 2019. https://doi.org/10.1109/TIE.2018.2835404

[9] Q. H. Tran, H. H. Lee, "An advanced modulation strategy for three-to-five-phase indirect matrix converters to reduce common-mode voltage with enhanced output performance", In IEEE Transactions on Industrial Electronics, Vol. 65, No. 7, pp. 5282-5291, July 2018. https://doi.org/10.1109/TIE.2017.2782242

[10] D. Casadei, G. Serra, A. Tani, "The use of matrix converters in direct torque control of induction machines", IEEE Trans. Ind. Electron., Vol. 4, pp. 1057-1064, 2001. https://doi.org/10.1109/IECON.1998.724186

[11] H. H. Lee, H. M. Nguyen, T. W. Chun, W. H. Choi, "Implementation of direct torque control method using matrix converter fed induction motor", 2007 International Forum on Strategic Technology, Ulaanbaatar, pp. 51-55, 2007. https://doi.org/10.1109/IFOST.2007.4798517

[12] H. Dan, P. Zeng, W. Xiong, M. Wen, M. Su, M. Rivera, "Model predictive control-based direct torque control for matrix converter-fed induction motor with reduced torque ripple", CES Transactions on Electrical Machines and Systems, Vol. 5, No. 2, pp. 90-99, June 2021. https://doi.org/10.30941/CESTEMS.2021.00012

[13] J. Monteiro, J. F. Silva, S. F. Pinto, J. Palma, "Matrix converter-based unified power-flow controllers: advanced direct power control method", IEEE Trans. Power Deliv., Vol. 26, No. 1, pp. 420–430, 2011. https://doi.org/10.1109/TPWRD.2010.2055897

[14] X. Wang, Q. Guan, L. Tian, "A novel adaptive fuzzy control for output voltage of matrix converter", 2012 7th Int. Power Electronics and Motion Control Conf. (IPEMC), Harbin, People's Republic of China, Vol. 1, pp. 53–58, June 2012. https://doi.org/10.1109/IPEMC.2012.6258843

[15] C. F. Calvillo, F. Martell, J. L. Elizondo, A. Avila, M. E. Macias, M. Rivera, "Rotor current fuzzy control of a DFIG with an indirect matrix converter", IECON 2011-37th Annual Conf. on IEEE Industrial Electronics Society, Melbourne, VIC, Australia, pp. 4296–4301, November 2011. https://doi.org/10.1109/IECON.2011.6120014

[16] T. N. Mir, B. Singh, A. H. Bhat, "Predictive speed estimation for encoderless control of an induction motor fed by delta sigma modulated matrix converter", In IEEE Transactions on Industry Applications, Vol. 56, No. 6, pp. 6477-6485, November-December 2020. https://doi.org/10.1109/TIA.2020.3013722

[17] M. Rivera, P. Wheeler, A. Olloqui, D. Khaburi, "A review of predictive control techniques for matrix converters—Part I", In Proceedings of the 2016 7th Power Electronics

and Drive Systems Technologies Conference (PEDSTC), Tehran, Iran, 16–18, pp. 582–588, February 2016. https://doi.org/10.1109/PEDSTC.2016.7556925

[18] M. Rivera, P. Wheeler, A. Olloqui, "Predictive control in matrix converters—Part II: Control strategies, weaknesses and trends", In Proceedings of the 2016 IEEE International Conference on Industrial Technology (ICIT), Taipei, Taiwan, 14–17, pp. 1098–1104, March 2016. https://doi.org/10.1109/ICIT.2016.7474907

[19] S. Toledo, D. Caballero, E. Maqueda, J. J. Cáceres, M. Rivera, R. Gregor, P. Wheeler, "Predictive control applied to matrix converters: A systematic literature review", Energies, Vol. 15, No. 20, 2022. https://doi.org/10.3390/en15207801

[20] M. Khosravi, M. Amirbande, D. A. Khaburi, M. Rivera, J. Riveros, J. Rodriguez, A. Vahedi, P. Wheeler, "Review of model predictive control strategies for matrix converters", IET Power Electronics, Vol. 12, No. 12, pp. 3021-3032, 2019. https://doi.org/10.1049/iet-pel.2019.0212

[21] R. Vargas, J. Rodriguez, C. A. Rojas, M. Rivera, "Predictive control of an induction machine fed by a matrix converter with increased efficiency and reduced common-mode voltage", IEEE Transactions on Energy Conversion, Vol. 29, No. 2, pp. 473-485, June 2014. https://doi.org/10.1109/TEC.2014.2299594

[22] R. Vargas, J. Rodriguez, U. Ammann, P. W. Wheeler, "Predictive current control of an induction machine fed by a matrix converter with reactive power control", IEEE Transactions on Industrial Electronics, Vol. 55, No. 12, pp. 4362-4371, December 2008. https://doi.org/10.1109/TIE.2008.2006947

[23] L. Tarisciotti, J. Lei, A. Formentini, A. Trentin, P. Zanchetta, P. Wheeler, M. Rivera, "Modulated predictive control for indirect matrix converter", IEEE Transactions on Industry Applications, Vol. 53, No. 5, pp. 4644-4654, September-October 2017. https://doi.org/10.1109/TIA.2017.2699666

[24] Y. Liu, Y. Liu, B. Ge, H. Abu-Rub, "Interactive grid interfacing system by matrix-converter-based solid state transformer with model predictive control", IEEE Transactions on Industrial Informatics, Vol. 16, No. 4, pp. 2533-2541, April 2020. https://doi.org/10.1109/TII.2017.2679137

[25] J. Rodriguez, R. Pontt, R.Vargas, P. Lezana, U. Ammann, P. Wheeler, "Predictive direct torque control of an induction motor fed by a matrix converter", European Conf. on Power Electronics and Applications, Aalborg, Denmark, pp. 1–10, September 2007. https://doi.org/10.1109/EPE.2007.4417295

[26] M. López, J. Rodriguez, C. Silva, M. Rivera, "Predictive torque control of a multidrive system fed by a dual indirect matrix converter", IEEE Transactions on Industrial Electronics, Vol. 62, No. 5, pp. 2731-2741, 2015. https://doi.org/10.1109/TIE.2014.2364986

[27] M. Uddin, S. Mekhilef, M. Mubin, M. Rivera, J. Rodriguez, "Model predictive torque ripple reduction with weighting factor optimization fed by an indirect matrix converter", Electric Power Components and Systems, Vol. 42, No. 10, pp. 1059–1069, 2014. https://doi.org/10.1080/15325008.2014.913739

[28] S. Toledo, M. Rivera, P. Wheeler, T. Dragicevic, D. Caballero, R. Gregor, "Active and reactive power control based on an inner predictive voltage control loop for AC generation systems with direct matrix converter", 2019 IEEE International Autumn Meeting on Power, Electronics and Computing (ROPEC), Ixtapa, Mexico, pp. 1-6, 2019. https://doi.org/10.1109/ROPEC48299.2019.9057037

[29] S. Toledo, M. Ayala, E. Maqueda, R. Gregor, A. Renault, M. Rivera, "Active and reactive power control based on predictive voltage control in a six-phase generation system using modular matrix converters", 2020 IEEE International Conference on Industrial Technology (ICIT), Buenos Aires, Argentina, pp. 1059-1065, 2020. https://doi.org/10.1109/ICIT45562.2020.9067285

[30] M. Ortega, F. Jurado, J. Carpio, "Control of indirect matrix converter with bidirectional output stage for micro-turbine", IET Power Electron., Vol. 5, No. 6, pp. 659–668, 2012. https://doi.org/10.1049/iet-pel.2011.0210

[31] S. Yusoff, L. De Lillo, P. Zanchetta, P. Wheeler, "Predictive control of a direct AC/AC matrix converter power supply under non-linear load conditions", 2012 15th International Power Electronics and Motion Control Conference (EPE/PEMC), Novi Sad, Serbia, pp. DS3c.4-1-DS3c.4-6, 2012. https://doi.org/10.1109/EPEPEMC.2012.6397340

[32] M. Rivera, J. Rodriguez, J. R. Espinoza, H. Abu-Rub, "Instantaneous reactive power minimization and current control for an indirect matrix converter under a distorted AC supply", In IEEE Transactions on Industrial Informatics, Vol. 8, No. 3, pp. 482-490, August 2012. https://doi.org/10.1109/TII.2012.2194159

[33] C. F. Garcia, M. E. Rivera, J. R. Rodríguez, P. W. Wheeler, R. S. Peña, "Predictive current control with instantaneous reactive power minimization for a four-leg indirect matrix converter", In IEEE Transactions on Industrial Electronics, Vol. 64, No. 2, pp. 922-929, February 2017. https://doi.org/10.1109/TIE.2016.2610939

[34] M. Roostaee, B. Eskandari, M. R. Azizi, "Predictive current control with modification of instantaneous reactive power minimization for direct matrix converter", 2018 9th Annual Power Electronics, Drives Systems and Technologies Conference (PEDSTC), Tehran, Iran, pp. 199-205, 2018. https://doi.org/10.1109/PEDSTC.2018.8343796

[35] M. Rivera, J. Rodriguez, J. Espinoza, B. Wu, "Reduction of common-mode voltage in an indirect matrix converter with imposed sinusoidal input/output waveforms", IECON 2012 - 38th Annual Conference on IEEE Industrial Electronics Society, Montreal, QC, Canada, pp. 6105-6110, 2012. https://doi.org/10.1109/IECON.2012.6389083

[36] R. Vargas, U. Ammann, J. RodrÍguez, "Predictive approach to increase efficiency and reduce switching losses on matrix converters", In IEEE Transactions on Power Electronics, Vol. 24, No. 4, pp. 894-902, April 2009. https://doi.org/10.1109/TPEL.2008.2011907

[37] J. Rodriguez, P. Cortes, "Predictive control of power converters and electrical drives", John Wiley & Sons, 2012. https://doi.org/10.1002/9781119941446

[38] M. Nabizadeh, P. Hamedani, B. Mirzaeian Dehkordi, "A comparative evaluation of model predictive current controlled matrix converter versus AC-DC-AC converter", Journal of Electrical and Computer Engineering Innovations (JECEI), Vol. 13, No. 2, pp. 431-442, 2025. https://doi.org/10.22061/jecei.2025.11435.804

[39] B. Wen, X. Zhang, Q. Wang, R. Burgos, P. Mattavelli, D. Boroyevich, "Comparison of three-phase ac-ac matrix converter and voltage dc-link back-to-back converter topologies based on EMI filter", 2013 IEEE Energy Conversion Congress and Exposition, Denver, CO, USA, pp. 2698-2706, 2013. https://doi.org/10.1109/ECCE.2013.6647050

[40] M. Vijayagopal, L. Empringham, L. de Lillo, L. Tarisciotti, P. Zanchetta, P. Wheeler, "Control of a direct matrix converter induction motor drive with modulated model predictive control", 2015 IEEE Energy Conversion Congress and Exposition (ECCE), Montreal, QC, Canada, pp. 4315-4321, 2015. https://doi.org/10.1109/ECCE.2015.7310270

[41] P. Hamedani, C. Garcia, F. Flores-Bahamonde, S. Sadr, J. Rodriguez, "Predictive control of 4-level flying capacitor inverter for electric car applications", 2022 13th Power Electronics, Drive Systems, and Technologies Conference (PEDSTC), Tehran, Iran, pp. 224-229, 2022. https://doi.org/10.1109/PEDSTC53976.2022.9767266